Finite Element Analysis of Lumbar Spine (L3-L5) Loading under Pothole-Induced Vibration in Powered Two-Wheelers

Santosh Prasad[1*], Avadhoot Nadgouda[1], Khyati Verma[1], Abhilash Singh[1]

[1] **Department of Mechanical Engineering, National Institute of Technology Karnataka, Surathkal, India.**

(E-mail: santosh.243md002@nitk.edu.in, avadhootnadgouda.221me306@nitk.edu.in, kverma@nitk.edu.in, asingh@nitk.edu.in)

Abstract. Powered two-wheelers (PTWs) constitute a dominant mode of transport in India, yet prolonged exposure to road irregularities subject's riders to continuous whole-body vibration (WBV), increasing the risk of lower back pain (LBP). The present study investigates the biomechanical behaviour of the L3–L5 lumbar segment under pothole-induced loading using experimentally acquired vibration inputs. A three-dimensional CT-based lumbar model was reconstructed and analysed using finite element methods. Field measurements were conducted using an in-house triaxial inertial measurement unit mounted at the L4 level while traversing a standardized pothole at speeds of 10, 20, and 30 km/h. The recorded peak vertical accelerations were transformed into equivalent compressive loads for numerical evaluation. The predicted intradiscal pressure (IDP) at the L4–L5 disc ranged between 1.4293 and 2.5925 MPa, showing strong consistency with reference loading cases of 1000 N and 2000 N. The results confirm that real-world transient vibration peaks can be effectively approximated using peak-equivalent static loading. The developed framework offers a practical approach for assessing vibration-related spinal risk and evaluating mitigation strategies for PTW riders.

Keywords: Finite Element Model, Lumbar spine, Powered two-wheeler, Road-induced vibration.

1 Introduction

Low back pain (LBP) represents one of the most prevalent musculoskeletal disorders worldwide. Repeated exposure to vehicle-induced vibration has been identified as a contributing mechanical factor affecting spinal health [6]. In India, riders of powered two-wheelers (PTWs) are frequently exposed to whole-body vibration (WBV) transmitted from irregular road surfaces to the lumbar spine (L3–L5) through the seat–rider

S. Uppapalli and D. Chakraborty (eds.), *Proceedings of the International Conference on Mechanics, Materials and Mechatronics (ICM³ 2026)*, Atlantis Highlights in Engineering 47,
https://doi.org/10.2991/978-94-6239-764-4_7

interface. Field measurements under real riding conditions have demonstrated significant vertical accelerations at this interface. Unlike laboratory-generated excitations, road-induced vibrations are irregular, broadband, and intermittent in nature. Simple harmonic models cannot accurately represent this response, as they arise from complex interactions between vehicle and roads. Therefore, the lumbar spine (L3-L5) is of particular interest as it bears the 60% of the body weight [7] and is susceptible to fatigue and micro damage when excitation frequency matches the natural frequency of the spine 8-40 Hz [6].

For studying the response of the spinal biomechanics of complex loading conditions, finite element analysis (FEA) has become an essential method. Earlier studies relied on simplified geometries that excluded ligamentous structures and accurate disc profiles, limiting bio fidelity [8]. One incorporated non-linear material properties but utilized geometry that was not CT scans but focused on a single specimen with simplified disc ligament interactions [3]. This field was advanced by developing a whole-body MRI based model validated for resonant frequency, yet their material for simulation remains simplified by [1].

A critical gap in the literature exists in the study of potholes and the analysis of transient dynamic responses using real-world road data rather than theoretical sinusoidal inputs. Most of the studies failed to capture the random and varying characteristics of the actual potholes induces vibration in PTW. The novelty of this work lies in the integration of the real-world data; vibration profiles were calculated using in house-built setup to capture actual pothole induced vibration at different speeds. These real-time data were translated into static peak force to simulate the actual stress defect experienced on the lumbar spine during the ride events like pothole impact. By combining the lumbar (L3-L5) geometry with the data driven loading, this research aims to provide a reliable biomechanical baseline for evaluating the vibration induces risk injury in the lumbar region.

2 Materials and Methods

A three-dimensional L3–L5 spinal unit model, reconstructed from CT-based anatomical data obtained from an open-source repository (GrabCAD), was processed in SOLIDWORKS 2024 (Fig 1(a), (b) and (c), segmented into detailed vertebral and disc components. Model validation included static bending, compressive loading, modal, and random vibration analyses. Additionally, in-house triaxial accelerometer measurements recorded lumbar vibrations of a PTW rider traversing a 13 cm diameter, 4 cm deep pothole at 10, 20, and 30 km/h. The measured peak accelerations were converted into equivalent force inputs for compression analysis.

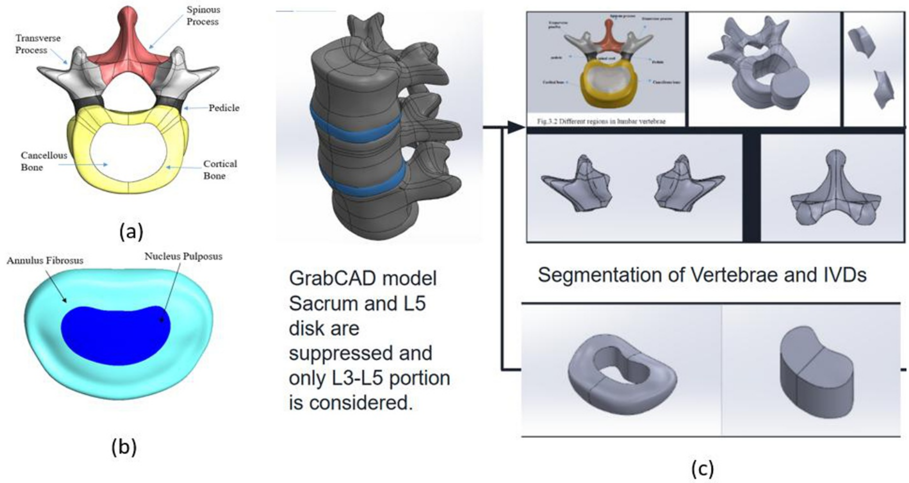

Fig.1. Frame work for the segmentation and FE analysis of L3-L5

2.1 Material properties

The material properties were assumed to be isotropic and linear elastic and were adopted from literature [1][2]. The material properties are shown in Table 1. Due to the complex geometric variation Quadratic Tetrahedral meshing was adopted. The FE model approximately included 707395 nodes and 475948 solid elements. Bonded contacts were considered between the segments of the vertebrae and the intervertebral disc (IVDs). A mesh convergence study was conducted to determine the appropriate mesh density, with validation deviation remaining within 10–12%, which is acceptable for complex biological finite element models.

Table 1. Material Properties [1][2]

Materials	Density (kg/mm^3)	Young's Modulus (MPa)	Poisson's Ratio	Element Type
Cortical Bone	1.7×10^{-6}	12000	0.3	10-node tetrahedral (C3D10)
Cancellous Bone	1.1×10^{-6}	100	0.2	10-node tetrahedral (C3D10)
Posterior Bone	1.0×10^{-6}	3000	0.3	10-node tetrahedral (C3D10)
Annulus Fibrosus	1.05×10^{-6}	4.2	0.45	10-node tetrahedral (C3D10)
Nucleus Pulposus	1.05×10^{-6}	1.0	0.49	10-node tetrahedral (C3D10)

3 Boundary Conditions

To validate the FE model, the model was assessed under static bending and axial compression scenarios. The applied boundary conditions were consistent with those considered by [1] and are summarized in Fig 2.

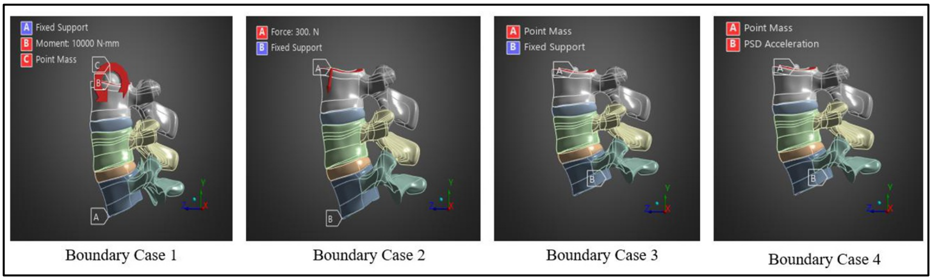

Fig. 2. Boundary conditions for different cases

Case 1: The inferior surface of L5 was constrained while prescribed bending moments 10 Nm and axial load of 40 kg point mass representing the upper body mass were applied on L3 for static analysis. Flexion, extension and lateral bending were in the direction in which the moment was applied. Computed range of motion (ROM) and intradiscal pressure (IDP) values were compared with previously published datasets. The predicted response demonstrated acceptable agreement, indicating appropriate representation of stiffness and load transfer characteristics within the lumbar segment.

Case 2: The inferior face of L5 was fixed and axial loads of 300N, 1000N and 2000N were applied at the top of the superior face of L3 for compressive validation under static loading. The mean intradiscal pressure (IDP) at the L4-L5 level was determined.

Case 3: For modal analysis of the L3–L5 segment, the inferior surface of L5 was constrained, and a 40 kg point mass representing the upper body was applied to the superior surface of L3. The first-order resonant frequency in the vertical direction (FRFV) was obtained by means of participation factor summary to the eigenvalue problem solution of modal analysis.

Case 4: This case's boundary conditions were identical to those of case 3. Furthermore, a random vibration excitation was applied in the vertical direction over the frequency range of 0-300 Hz, with a constant PSD acceleration of 0.05 m^2/s^3 (based on the natural frequency range derived from modal analysis).

4 Results and Discussion

4.1 Static Validation.

The Case 1 was used for the L3-L5 lumbar spine FE model, the ROM results for extension, flexion, left lateral bending, and right lateral bending at 10 Nm are shown in Table 2 and compared with those reported in [1]. The new model's findings showed difference and the minimum were 0.29% for the flexion ROM and maximum 93.71% for extension ROM. Since the extension value only shows a moderate level of agreement, the model needs further refinement.

Table 2. Comparison of IVD level under the bending load condition

Bending Moment direction	IVD Level	This Study (°)	Guo & Zhang [1] (2022) (°)	Difference (%)
Flexion ROM (°)	L3–L4	+6.78	+6.8	-0.29
	L4–L5	+7.05	+8.9	-20.79
Extension ROM (°)	L3–L4	−6.78	−3.5	+93.71
	L4–L5	−7.05	−5.4	+30.56
Left Lateral Bending Moment ROM (°)	L3–L4	−4.71	−5.5	-14.36
	L4–L5	−4.26	−5.0	-14.80
Right Lateral Bending Moment ROM (°)	L3–L4	+4.71	+5.4	-12.78
	L4–L5	+4.26	+5.0	-14.80

To confirm the compressive pressure of IVDs, the average IDP results for L4-L5 were obtained (Case 2) and compared with the literature [1]. The current model's values under axial compression stresses of 300 N, 1000 N, and 2000 N were 0.23 MPa, 0.78 MPa, and 1.55 MPa, respectively, which showed excellent agreement with reference values. The IDP value comparison at the L4-L5 level is displayed in Table 3.

Table 3. Comparison of average IDP at L4-L5 IVD under compressive loading

Compressive Load (N)	Avg. IDP at L4-L5 IVD (MPa) (This Study)	Avg. IDP at L4-L5 IVD (MPa) [1]
300	0.23	0.23
1000	0.78	0.78
2000	1.56	1.55

4.2 Dynamic Validation

Modal analysis of the L3-L5 segment was conducted to validate the dynamic response of the lumbar spine model in case 3. The natural frequencies, obtained as the solution to the eigenvalue problem, ranged from 3.35 Hz to 281.41 Hz. Eigenvalue analysis was performed to determine the inherent dynamic characteristics of the segment. The dominant vertical resonance mode was identified at approximately 19.7 Hz based on effective mass participation factors. This frequency lies within the typical resonance range reported for lumbar structures, confirming the model's dynamic fidelity. Subsequent in case 4 frequency-domain excitation was applied to evaluate the acceleration response under broadband vertical input. Fig 3(a) and Fig 3(b) displayed the acceleration power spectral density (PSD) response curve in the vertical direction under the random vibration excitation, as well as the first-order vibration mode in the vertical direction (FVMV) of the lumbar spine .

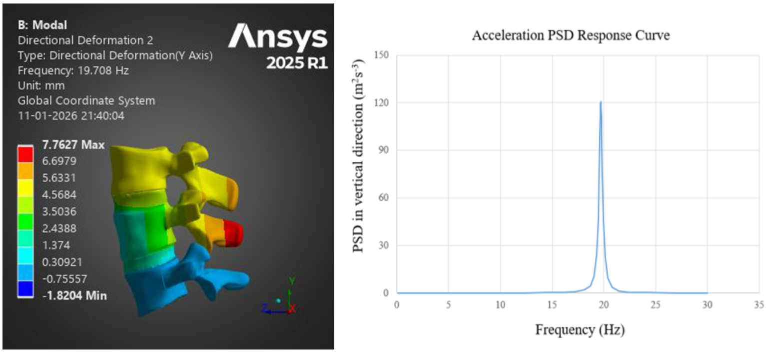

(a) (b)

Fig 3. (a) Displacement in vertical direction corresponding to FRFV (FVMV), (b) PSD curve acceleration under random vibration excitation in a vertical direction

4.3 Structural analysis under peak acceleration recorded by the sensor

Three trials with the peak accelerations in the vertical direction were recorded for a 50th percentile Indian male rider of mass 74 kg. The equivalent upper body weight contributing to lumbar loading 44.4 kg (60% of total body weight) was considered and the calculated peak force was used to find the average IDP at the L4-L5 IVD.

Table 4. Loading conditions along with the corresponding speed, peak acceleration, duration and equivalent compressive load, average IVD pressure

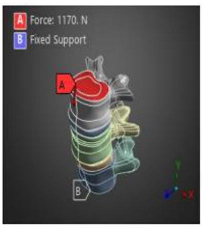	Vehicle speed (kmph)	Peak acceleration in vertical direction in g (ms^{-2})	Duration (m s)	Equivalent compressive Force (N)
	10	7.60	48	3310.3
	20	6.00	12	2613.4
	30	4.19	13	1825

Table 5. Based on the applied compressive force the average IVD pressure as mentioned above (Table 4).

Compressive Force (N)	Avg. IDP at L4-L5 IVD (MPa)
3310.3 (at 7.6g acceleration)	2.5925
2613.4 (at 6g acceleration)	2.0467
1825 (at 4.19g acceleration)	1.4293

The mean stress distribution of the IVD at different compressive force is taken and the results shows that with the increase in the external loading conditions internal stress also increases within the IVD as shown in Fig. 4.

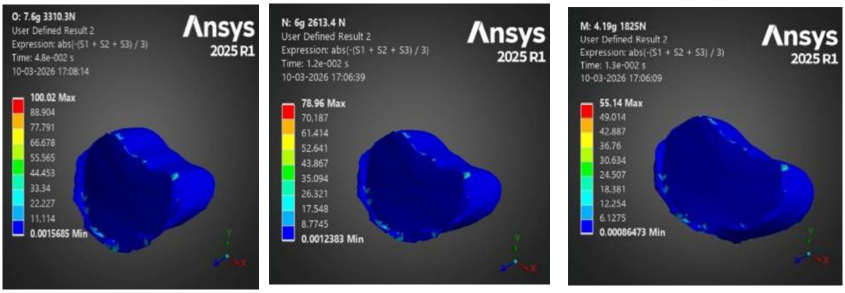

Fig 4. Mean stress distribution at different loads (a) 7.6g, (b) 6g & (c) 4.19g.

5 Discussion

The primary aim of this investigation was to construct a biomechanically consistent computational representation of the L3–L5 segment and to examine its response under experimentally derived vibration loading. Geometric segmentation was conducted based on anthropometric data; minor variations (<5%) were attributed to the specific subject anatomy of the open-source model but remained within reasonable ranges.

Static and Dynamic Validations: The generated FE model's prediction performance under axial compression was confirmed by the static validation findings, which showed strong agreement with previously reported experimental data. The findings of the extension and lateral bending range of motion (ROM) showed greater variations. These variations can be explained by the reconstructed geometry's simplifications, such as the segmented model's integration of facet joint areas and the lack of endplates, which affect spinal flexibility under bending stresses. Additionally, compared to reference studies, the bending response might have been impacted by the application of the upper-body mass as a concentrated load on the superior vertebral surface. However, as shown in Table 3, the compressive validation demonstrated outstanding agreement with published intradiscal pressure data, which is crucial for the current study. In addition, whole body vibration mainly acts in the vertical direction; therefore, the lateral bending behaviour of the spine might have little impact on the results of the response. Dynamic validation identified the First-order Resonant Frequency in the Vertical direction (FRFV) at 19.7 Hz. This aligned closely with the findings of (19.4–19.6 Hz), with the Power Spectral Density (PSD) curve peak confirming the critical resonant frequency reported [1].

Structural Analysis under Vibration-Induced Loading: Static analysis of the spine under vibration-induced peak forces (speed hump) indicated that the highest stress concentrations occurred in the pedicle and spinal canal regions. These areas are structurally predisposed to high stress due to the smaller thickness of the pedicle and the sharp corner geometry of the spinal canal relative to the vertebral body. Consequently, these regions are identified as the most vulnerable to acute stress fractures under high-impact vertical loading.

6 Conclusions

This study quantified the biomechanical response of the L3–L5 lumbar spine to pothole induced vibration loading during powered two-wheeler riding using a validated finite element model. The predicted intradiscal pressure at the L4–L5 level increased with impact severity and at 30km/h the impact is within the limit of 1000 and 2000 N but the impact severity is more at 10 & 20km/h due to the time duration of the impact and it exceeds the safe limit of the physiological range. The results demonstrate that transient road-induced vibrations can impose significant lumbar loading, contributing to the risk of lower back pain among riders. The validated modeling approach reliably represents real-world riding conditions idealized as static peaks and provides a useful framework for evaluating vibration mitigation strategies, ergonomic interventions, and road-induced spinal injury risk.

Acknowledgments. The author would sincerely thank the Department of Mechanical Engineering, National Institute of Technology Karnataka, for providing the funds and research facilities required to complete my work, and would also like to thank my supervisor, Dr Khyati Verma, for her supervision and advice throughout the research.

References

1. Zhang, C., Guo, L.-X.: Effect of whole-body vibration at different frequencies on the lumbar spine: A finite element study based on a whole human body model. *Proceedings of the Institution of Mechanical Engineers, Part H: Journal of Engineering in Medicine* **236**(12), 1752–1761 (2022)
2. Sahani, R.: Finite element analysis of L2–L4 lumbar spine segment with and without fixation. Master's thesis, Indian Institute of Technology Delhi, India (2015)
3. Poojara, R.K., Keshri, A.K., Kumar, R.: Biomechanical response of L4–L5 lumbar spine segment under different physiological loading conditions: A finite element study. *Materials Today: Proceedings* **44**, 4391–4396 (2021)
4. Garavelli, C., Wyers, C.E., van der Linden, J.C., van Rietbergen, B., Ito, K.: A subject-specific finite element model of the metastatic spine validated against digital image correlation measurements. *Journal of the Mechanical Behaviour of Biomedical Materials* **126**, 105028 (2022)
5. Wiczenbach, T., Dąbrowski, P., Mazurkiewicz, A.: Validation of the THUMS L1–L5 lumbar spine finite element model under pure moment loading. *Applied Sciences* **13**(3), 1542 (2023)
6. Jain, A.R.T., Tony, B., Alphin, M.S., Sri Krishnan, G.: Simulation of L4 lumbar spine model of motorist exposed to vibration from speed hump. *Journal of Orthopaedics* **22**, 390–396 (2020)
7. Wang, S., Park, W.M., Kim, Y.H., Cha, T., Wood, K., Li, G.: In vivo loads in the lumbar L3–4 disc during a weight-lifting extension. *Clinical Biomechanics* **29**(2), 155–160 (2014)
8. Divya, V., Anburajan, M.: Finite element analysis of human lumbar spine. In: *Proceedings of the IEEE International Conference on Biomedical Engineering*, pp. 350–354. IEEE (2011)